PNAS
www.pnas.org

Supplementary Information for

Metastable quasicrystal-induced nucleation in a bulk glass-forming liquid

Güven Kurtuldu [1,*], Karl F. Shamlaye [1] and Jörg F. Löffler [1,*]
[1] Laboratory of Metal Physics and Technology, Department of Materials, ETH Zurich, 8093 Zurich, Switzerland

*Güven Kurtuldu, *Jörg F. Löffler
Email: guven.kurtuldu@mat.ethz.ch, joerg.loeffler@mat.ethz.ch

This PDF file includes:

Figs. S1 to S6
Table S1
References for SI reference citations

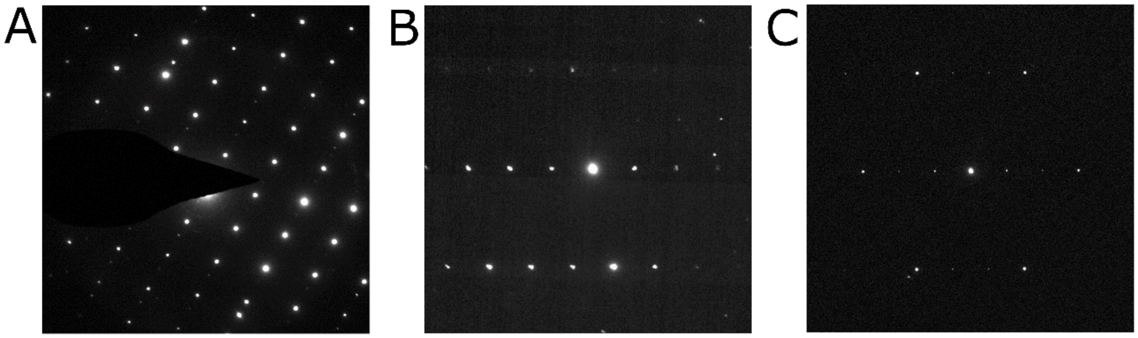

Fig. S1. Diffraction pattern of $Mg_{51}Zn_{20}$-type phase. Selected area diffraction patterns of the microstructure in as-cast $Mg_{64}Zn_{27}Yb_9$ shown in Figure 2c along (*A*) [201], (*B*) [250] and (*C*) [034] zone axes of $Mg_{51}Zn_{20}$-type phase (orthorhombic, Immm, *a* = 14.083 Å, *b* = 14.486 Å, *c* = 14.025 Å) (1) with modified lattice parameters (*a* = 13.707 Å, *b* = 14.819 Å, *c* = 14.047 Å).

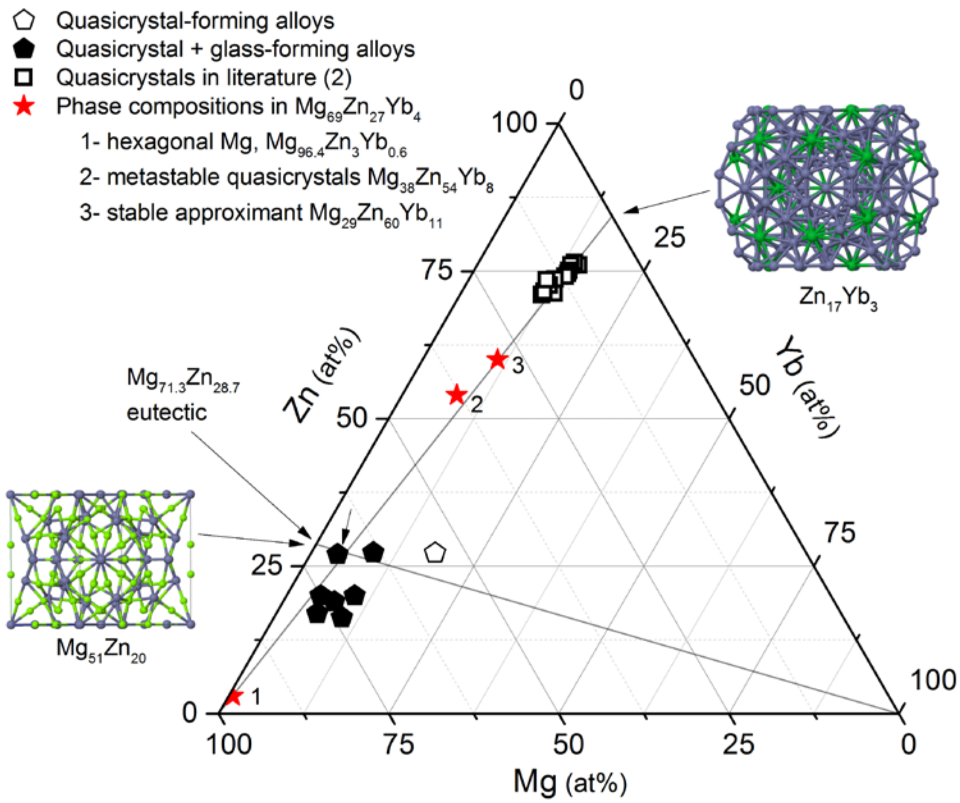

Fig. S2. Mg–Zn–Yb compositions. Mg–Zn–Yb ternary diagram indicating compositions for: QC and metallic glass-forming alloys found in this study; QC-forming alloys investigated by Mitani and Ishimasa (2); binary approximant phases: $Mg_{51}Zn_{20}$ (3, 4), $Zn_{17}Yb_3$ (5); and constructed cluster lines binding $Zn_{17}Yb_3$ to Mg and eutectic composition $Mg_{71.1}Zn_{28.9}$ (6) to Yb. The approximant phase $Mg_{29}Zn_{60}Yb_{11}$ "3" and the iQC phase $Mg_{38}Zn_{54}Yb_8$ "2" follow the cluster line between $Zn_{17}Yb_3$ and Mg. The $Mg_{69}Zn_{27}Yb_4$ alloy composition (see arrow) is located near the intersection of these two cluster lines and forms a BMG.

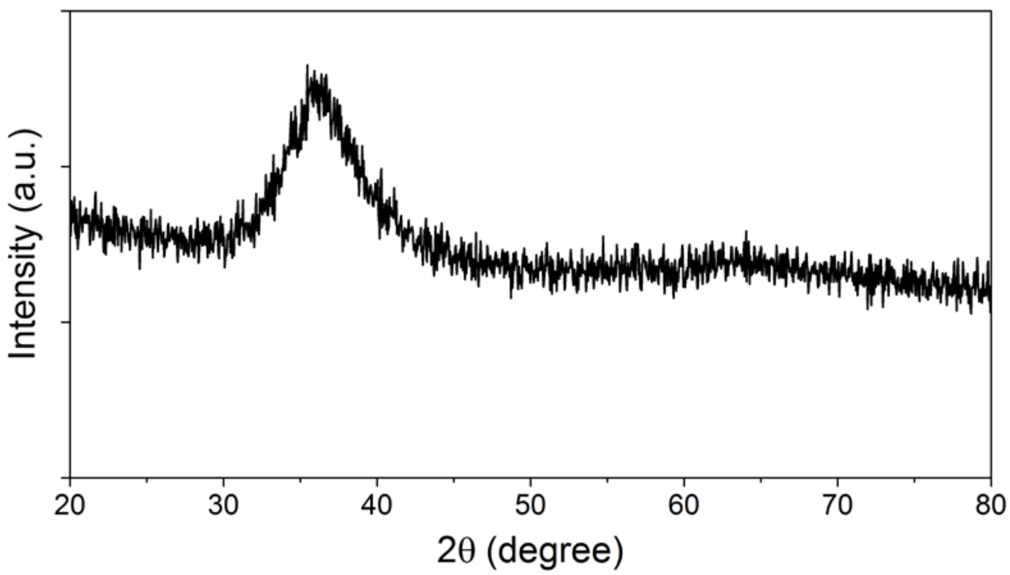

Fig. S3. XRD pattern of a $Mg_{69}Zn_{27}Yb_4$ bulk metallic glass. XRD pattern taken with Cu Kα radiation from the cross-sectional surface of a $Mg_{69}Zn_{27}Yb_4$ rod cast to 1 mm diameter.

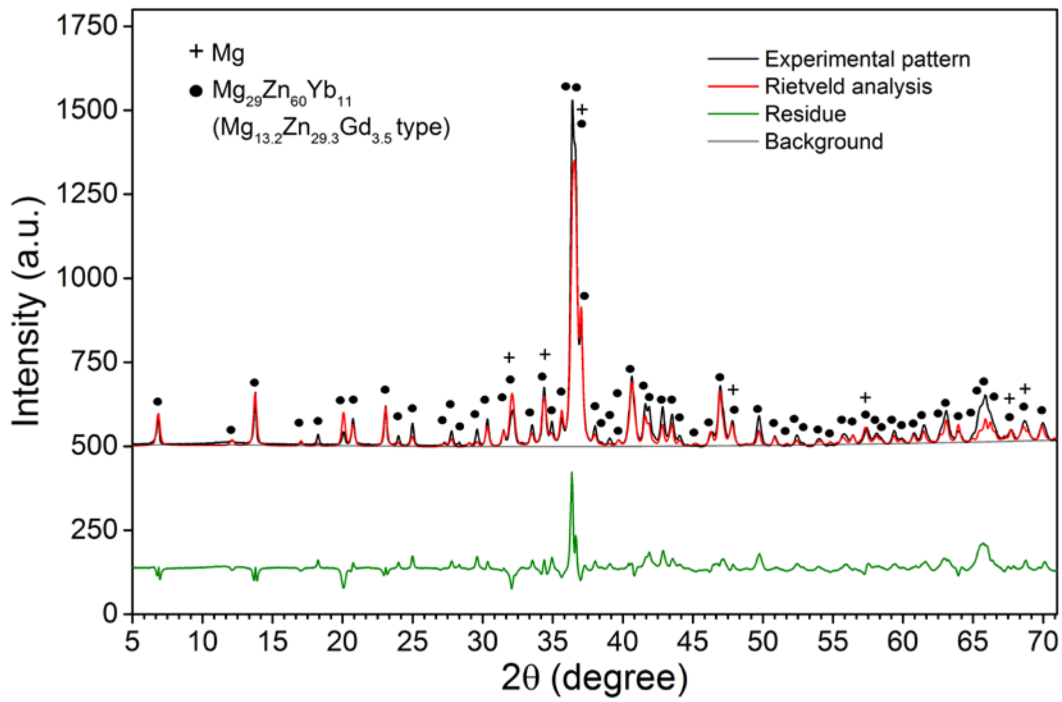

Fig. S4. XRD pattern of stable equilibrium state. XRD pattern taken with Cu Kα radiation for a $Mg_{69}Zn_{27}Yb_4$ alloy solidified at a cooling rate of 20 K/min using DSC. Diffraction peaks are indexed as Mg (hexagonal, P63/mmc, space group 194, a=b=3.2107 Å, c=5.2061 Å) and $Mg_{13.2}Zn_{29.3}Gd_{3.5}$-type $Mg_{29}Zn_{60}Yb_{11}$ phase (hexagonal, P63/mmc, space group 194, a=b=14.8053 Å, c=8.8256 Å). Rietveld analysis was performed using reference Mg crystal structure (ICDD reference code 04-003-5224, a=b=3.2040 Å, c=5.2070 Å) and $Mg_{13.2}Zn_{29.3}Gd_{3.5}$ crystal structure (ICDD reference code 04-009-2178, a=b=14.6330 Å, c=8.7610 Å).

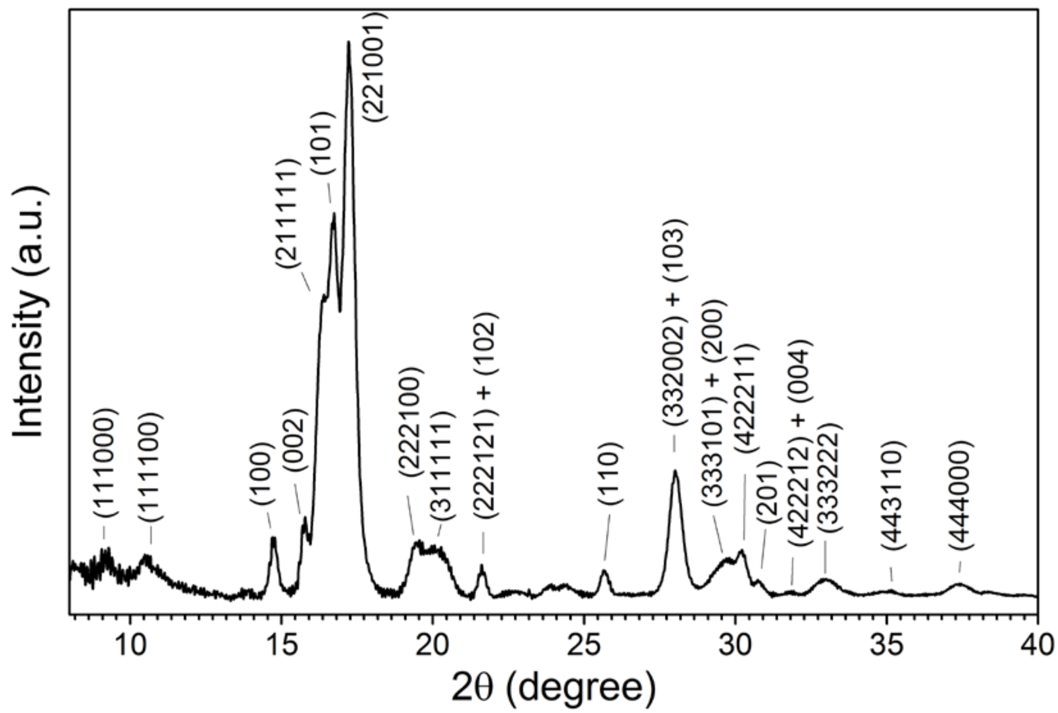

Fig. S5. XRD pattern of metastable state. XRD pattern taken with Mo Kα radiation for a $Mg_{69}Zn_{27}Yb_4$ alloy solidified at a cooling rate of 100 K/s using FDSC. Diffraction peaks are indexed as hexagonal Mg and primitive-type iQC; see Table S1.

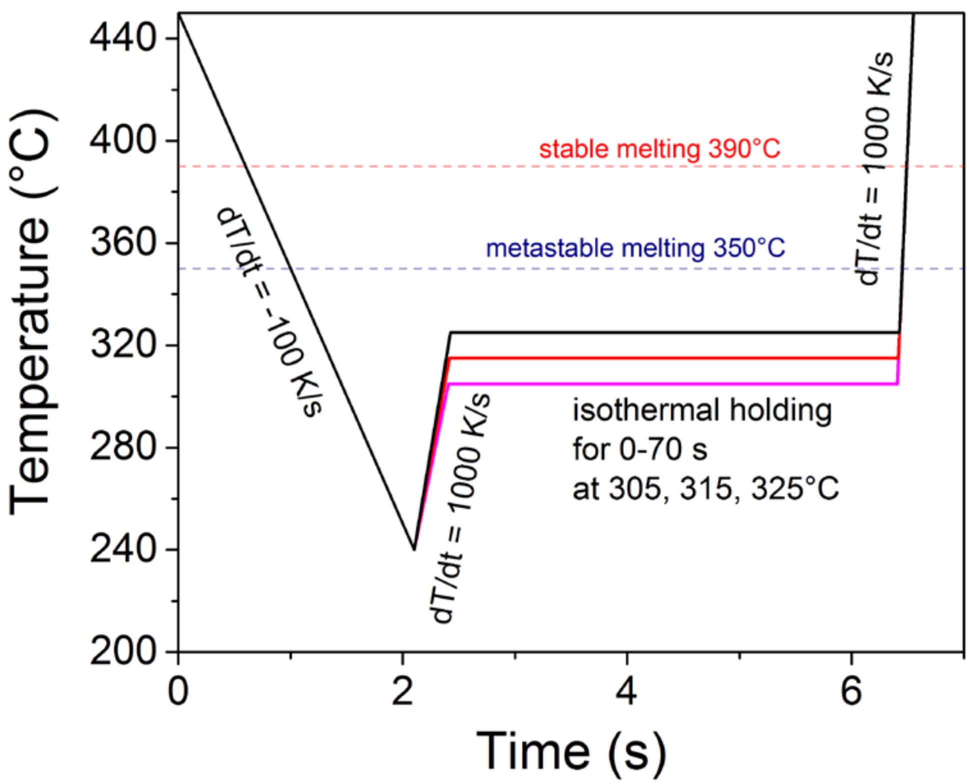

Fig. S6. Temperature profiles for studying the metastable-to-stable transition. The effect of temperature and time on the metastable-to-stable phase transition was investigated by designing FDSC experiments using the illustrated temperature profiles. $Mg_{69}Zn_{27}Yb_4$ melt is solidified at a cooling rate of 100 K/s, which results in formation of metastable QC and Mg phases. Cooling is interrupted at 240°C and the temperature of the metastable solid is increased to isothermal treatment temperatures (305, 315, 325°C) at a rate of 1,000 K/s. The metastable solid is then held at these temperatures for various time intervals (0–70 s), which generates a metastable-to-stable phase transition. Finally, the alloy is melted at a rate of 1,000 K/s.

Table S1. XRD peak positions for metastable state. Peak positions (2θ, *d*) and normalized peak intensities of hexagonal Mg and Mg–Zn–Yb primitive-type iQC formed during solidification in FDSC at a rate of 100 K/s, determined from XRD data (see Fig. S5). Peaks for the QC phase are indexed following the work of Elser (7) and distances are calculated using the six-dimensional lattice parameter a_{6D} = 7.46Å.

Index (QC)	Index (Mg)	2θ (Mo)	$d_{measured}$(Å)	$d_{calculated}$ (Å)	Δ*d* (Å)	Intensity
(111000)		9.23	4.416	4.425	0.009	7
(111100)		10.49	3.888	3.833	0.055	7
	(100)	14.74	2.771			9
	(002)	15.78	2.589			13
(211111)		16.41	2.490	2.491	0.001	55
	(101)	16.72	2.444			69
(221001)		17.23	2.372	2.369	0.003	100
(222100)		19.46	2.103	2.088	0.015	9
(311111)		20.40	2.007	2.015	0.008	9
(222121)	(102)	21.62	1.895	1.882	0.013	5
	(110)	25.66	1.600			4
(332002)	(103)	28.02	1.468	1.464	0.004	23
(333101)	(200)	29.72	1.386	1.390	0.004	7
(422211)	(112)	30.19	1.365	1.368	0.003	8
	(201)	30.92	1.339			5
(422212)	(004)	31.96	1.297	1.307	0.010	2
(333222)		32.99	1.252	1.243	0.009	3
(443110)		35.00	1.182	1.182	0.000	1
(444000)		37.39	1.109	1.106	0.002	2

References

1. Higashi I, Shiotani N, Uda M, Mizoguchi T, Katoh H (1981) The crystal structure of Mg51Zn20. *J Solid State Chem* 36(2):225–233.

2. Mitani T, Ishimasa T (2006) A metastable icosahedral quasicrystal in the Zn-Mg-Yb alloy system. *Philos Mag* 86(3–5):361–366.

3. Uchida M, Matsui Y (2002) The pseudocubic approximant Mg51Zn20 interpreted as a modulated crystal. *Philos Mag a Phys Condens Matter Struct Defects Mech Prop* 82(4):831–839.

4. Villars P, Cenzual K eds. Mg51Zn20 Crystal Structure: Datasheet from “PAULING FILE Multinaries Edition – 2012” in SpringerMaterials (http://materials.springer.com/isp/crystallographic/docs/sd_1826458).

5. Villars P, Cenzual K eds. Yb3Zn17 (Zn73.42Yb12.52) Crystal Structure: Datasheet from “PAULING FILE Multinaries Edition – 2012” in SpringerMaterials (http://materials.springer.com/isp/crystallographic/docs/sd_0251112).

6. Villars P, Okamoto H eds. Mg-Zn Binary Phase Diagram 0-100 at.% Zn: Datasheet from “PAULING FILE Multinaries Edition – 2012” in SpringerMaterials (http://materials.springer.com/isp/phase-diagram/docs/c_0904724).

7. Elser V (1985) Indexing problems in quasicrystal diffraction. *Phys Rev B* 32(8):4892–4898.